RasV12 Expression in Microglia Promotes Retinal Inflammatory Circuits and Impairment of Photoreceptor

Yuta Moriuchi
Div Mole Dev Biol, Inst Med. Sci, Univ. Tokyo
Toshiro Iwagawa
Div. Mol.Dev. Biol, Inst.Med.Sci, Univ.Tokyo
Asano Tsuhako
Inst.Med.Sci, Univ. Tokyo
Hideto Koso
Inst.Med.Sci.,Univ.Tokyo
Yasuyuki Fujita
Graduate school of Medicine, Kyoto Univ
Sumiko Watanabe (sumiko@ims.u-tokyo.ac.jp)
Institute of Medical Science, University of Tokyo https://orcid.org/0000-0003-4497-5750

Research

Keywords: microglia, retina, RasV12, transgenic mice, cytokines, phagocytosis

Posted Date: May 27th, 2020

DOI: https://doi.org/10.21203/rs.3.rs-29744/v1

Abstract

Background Microglial activation is commonly observed in neurodegenerative diseases. However, its role in the complex inflammatory network remains unclear. In this study, we generated a microglial activation mouse model by inducing the expression of a constitutively active form of Ras in microglia.

Methods The double transgenic lines *CAG-LSL-RasV12-IRES-EGFP; Cx3cr1*^{CreER} (Cx3cr1-RasV12 mice) and *CAG-LSL-EGFP;Cx3cr1*^{CreER} (control mice) were generated. The expression of RasV12 was induced in microglia by tamoxifen administration. Effects of the expression of RasV12 in the retina were examined by immunohistochemistry of frozen sections, RT-qPCR, and live imaging.

Results RasV12 expression in retinal microglial cells promoted cell proliferation, cytokine expression, and phagocytosis. RasV12-expressing microglia migrated towards the apical and basal regions of the retina. Examination of GFAP expression revealed activation of Müller glia in the retina. We also observed loss of the photoreceptors in the outer nuclear layer (ONL) in close proximity to microglial cells. However, no neurodegeneration was observed in the inner nuclear layer (INL) or ganglion cell layer (GCL). Furthermore, we found that RasV12-expressing microglia in the ONL were smaller in size and engulfed photoreceptors. In contrast, the morphology of RasV12-expressing microglia in the GCL and INL resembled resting microglia. In conclusion, RasV12-induced microglial activation impaired rod photoreceptor survival in the ONL, but not in other regions of the retina.

Conclusion The expression of RasV12 is sufficient to activate microglia, and our results suggested that microenvironment cues may modulate the microglial phenotypic features and effects of microglial activation.

Background

Microglia are tissue-resident macrophage-like cells, found throughout the central nervous system (CNS). Microglia play central roles in orchestrating immune responses in the CNS [1]. Recent evidence also suggests that microglia are involved in the pathogenesis of diseases associated with neuronal cell death through phagocytosis and secretion of inflammatory cytokines [2]. Therefore, the development of strategies to modulate microglial activities has emerged as a promising approach to treat neurodegenerative diseases.

Microglia have also been implicated in several pathological conditions in the retina, including glaucoma and photoreceptor degeneration. Under physiological conditions, retinal microglia display ramified morphologies, and are primarily found in the inner plexiform layer (IPL) and the outer plexiform layer (OPL). During development, retinal microglia promote neuronal cell survival by secreting neurotrophic factors and maintaining synaptic structures [3]. Retinal photoreceptor degeneration is accompanied with microglial activation. Upon activation, microglial cells undergo morphological alterations, acquiring ameboid shapes. Activated microglial cells migrate to the site of degeneration, the outer nuclear layer (ONL), and subretinal regions (SR) [4, 5]. Several studies demonstrated the critical role of microglia in the

onset and progression of retinal degeneration, by exerting neurotoxic effects upon activation. In the rd10 mouse model, microglial activation promoted photoreceptor apoptosis in an IL-1β-dependent manner, aggravating retinal degeneration [6]. Consistently, administration of minocycline ameliorated retinal degeneration in the rd10 mouse model [7]. However, the elucidation of the role of microglia in photoreceptor degeneration remains challenging due to the complexity of the retinal structure and immunological circuits involved in retinal diseases. Rod photoreceptors secrete alarmins, such as EDN2 [8]. Alarmins and other cytokines activate Müller glial cells (MGCs), which upon activation, secrete various cytokines, including leukemia inhibitory factor (LIF) [9, 10]. Furthermore, the retinal pigment epithelium (RPE) is often involved in immune responses under pathological conditions [11], further increasing the complexity of the mechanisms underlying retinal inflammation.

Ras is a central signal transducer, functioning as a GDP/GTP-regulated molecular switch (GTPase). Ras activation triggers several downstream signaling pathways, including the RAF/MEK/ERK cascade. The Ras superfamily consists of various related proteins; H-Ras, N-Ras, and K-Ras4A/B are the most common Ras proteins in mammals [12]. K-Ras is activated by various transmembrane receptors that induce microglial activation, including CSF1 receptor (CSF1R), Fc gamma receptor (FcγR), and TREM2 [13–15]. Aberrant Ras activation promotes oncogenesis, and Ras mutations have been identified in a wide variety of human cancers [12]. Substitution of G12 with V in H-Ras (H-RasV12) results in a constitutively active form, which was first described in epithelial cancer. The serine/threonine kinase BRAF is one of the oncoproteins that are activated by Ras. A recent study showed that microglial expression of a constitutively active form of BRAF, BRAFV600E, promoted microglia expansion and late-onset neurodegeneration in the brain [16].

The aim of this study was to investigate the effects of microglial RasV12 expression in the retina. We found that RasV12 expression promoted microglial cell proliferation and migration to all regions of the retina, accompanied by aberrant MGC activation. We also found that microglial cell migration to the ONL was accompanied by photoreceptor degeneration.

Methods

All experiments adhere with the declaration of Helsinki. All animal experiments were approved by the Animal Care Committee of the Institute of Medical Science, University of Tokyo and conducted in accordance with the Guidelines laid down by the NIH in the US regarding the care and use of animals for experimental procedures and the ARVO (Association for Research in Vision and Ophthalmology) statement for the use of animals in ophthalmic and vision research.

Mice strain, genotyping and tamoxifen treatment

B6.129P2(C)-*Cx3cr1*$^{tm2.1(cre/ERT2)Jung}$/J (*Cx3cr1*^{CreER}) was purchased from Jackson laboratory. To express RasV12 and EGFP in the microglia, we crossed the *Cx3cr1*^{CreER} mice [17], in which Cre-ER fusion protein encoding DNA was knock-in in into Cx3cr1 allele, with the *CAG-LSL-RasV12-IRES-Egfp* strain [18]

or *CAG-LSL-Egfp mice* [19]. The double transgenic line *Cx3cr1*^{CreER}; *CAG-LSL-RasV12-IRES-EGFP* was denoted as Cx3cr1-RasV12 mice and *Cx3cr1*^{CreER}; *CAG-LSL-EGFP* as control. Genotyping of Cx3cr1-RasV12 mice and Control mice was performed by PCR. The sequences of the primers are as follows; Cre-F 5'-tctagcgttcgaacgcactga-3' Cre-R 5'-caccatttttttctgaccc g-3', LSL-GFP-F 5'-cagtcagttgcacaat-3', LSL-GFP-R 5'-atatcaccagctcaccgtctt-3', RasV12-F 5'-cactgtggaatctcggcagg-3', RasV12-R 5'-gcaatatggtgaaaataac-3'. Fifty µl of Tamoxifen dissolved in cone oil (20 mg/ml, Sigma-Aldrich) was injected subcutaneously into Cx3cr1-RasV12 mice and control mice at postnatal day 14. Mice were harvested at 1,3,5, and 7 days post-injection.

Hematoxylin and Eosin (HE) staining

Brain and retina were isolated after perfusion fixation using 4% PFA in PBS and fixed overnight in the same solution at 4 °C. The samples were embedded into paraffin, and sectioned (4 µm). After deparaffinization, the sections were stained with Hematoxylin solution (FUJIFILM Wako Pure Chemical) for 10 min and washed by water for 30 min and stained with Eosin (MUTO PURE CHEMICALS). The sections were washed by ethanol for 20 min and then xylene for 15 min and mounted using Malinol (MUTO PURE CHEMICALS).

Immunohistochemistry

Immunohistochemistry of frozen sectioned retinas was performed as previously described [20]. Brain was isolated after perfusion fixation using 4% paraformaldehyde (PFA) and fixed overnight in 4 °C in 4% PFA. Fixed brains were subjected to sucrose replacement in 10% sucrose in PBS, followed by 25% sucrose in PBS. Thickness of the sections was either 10 or 16 µm. Primary antibodies are mouse anti-Brn3b (1:500, Santa Cruz Biotechnology), -AP-2α (1:50, DSHB), -iNOS(1:500, Novus), -GFAP (1:400, Sigma-Aldrich), -pERK1/2 (1:500, Cell Signaling Technology), -Rhodopsin (1:200, LSL), Ki67 (1:100, BD Pharmingen), rat anti-CD68 (1:2000, BIO-RAD), rabbit anti-Calbindin (1:500), Iba1 (1:1000, FUJIFILM Wako Pure Chemical), Recoverin (1:1000 Abcam), active Caspase3 (1:250, Promega), -Tmem119 (1:250, Abcam), sheep anti-Chx10 (1:500, EXALPHA), and chicken anti-GFP (1:2000, Abcam). The first antibodies were visualized by appropriate fluorescent second antibodies (Alexa Fluor® 488, 594 or 680, Thermo Fisher Scientific). Stained sections were observed by Axio Imager M1 microscope (Carl Zeiss) or Axio Imager M2 microscope (Carl Zeiss) with AxioVison ver.4.9.1.0 software (Carl Zeiss). Orthogonal images were taken by LSM710 confocal microscope (Carl Zeiss). Z-stacked images were taken at intervals of 1 µm with ZEN 2009- and ZEN 2.3 lite-software (Carl Zeiss).

Ex vivo confocal time-lapse imaging

Isolated retinas of Cx3cr1-RasV12 mice were placed on Millicell chamber filters (Millipore) and stained with 0.01 mg/ml of Hoechst33342 (DOJINDO LABORATORIES) for 10 min at room temperature. Then, the retinas were embedded in 1% agarose (NIPPON GENE) in PBS at 37 °C, and after agarose has the property of being solid, the filters were carefully removed from embedded retinas, and then the samples were served to the time-lapse imaging. The images were taken at 1 min interval, 90 times by LSM710

confocal microscope (Carl Zeiss). Images were edited using ZEN 2009 and ZEN 2.3 lite software (Carl Zeiss).

Flow cytometry

Isolated retains were dissociated to single cell level as described previously [20]. Peripheral blood were collected from tail vein, and the erythrocytes were lysed using ACK lysing buffer (Thermo Fisher Scientific). Cells were stained with PE-conjugated anti-CD11b antibody (Bio Legend), Alexa Fluor647-conjugated anti-CD73 antibody (BD Biosciences), or Annexin V-PE (Bio Vison). Dead cell exclusion was done by using propidium iodide (Sigma-Aldrich). Cells were analyzed by FACS Calibur (BD Biosciences). Data analysis were performed using Flow Jo software (BD Biosciences).

RT-qPCR

Total RNA was purified from mouse whole retina using Sepasol (Nacalai Tesque), and cDNA was synthesized using ReverTra Ace qPCR RT Master Mix (TOYOBO). Quantitative PCR (qPCR) was performed using the THUNDERBIRD SYBR qPCR Mix (TOYOBO) and the Roche Light Cycler 96 (Roche Diagnostics). *Actb* and *Sdha* were used as reference genes.

Statistical analysis

P-values were calculated by unpaired t-test.

Results

Generation of mice with inducible RasV12 expression in microglia

The double transgenic lines *CAG-LSL-RasV12-IRES-EGFP; Cx3cr1*^{CreER} (Cx3cr1-RasV12 mice) and *CAG-LSL-EGFP;Cx3cr1*^{CreER} (control mice) were used in this study. The chemokine receptor CX3CR1 is specifically expressed in monocytes and tissue-resident macrophages, including microglia [21]; hence, *Cx3cr1 CreER* knock-in mice expressed tamoxifen-inducible Cre recombinase in microglial cells. EGFP was also expressed after tamoxifen administration in both Cx3cr1-RasV12 mice and control mice, allowing for lineage tracing.

Control and Cx3cr1-RasV12 mice were born at the expected Mendelian ratio (Table 1). Tamoxifen was administered to control and Cx3cr1-RasV12 mice at postnatal day 14 (P14). Death of unknown causes was observed in Cx3cr1-RasV12 mice 9–10 days after tamoxifen injection. Since *Cx3cr1* is also expressed in circulating monocytes [21, 22], we evaluated the presence of monocytes with Cre-mediated recombination in the peripheral blood by flow cytometry (Supplementary Fig. S1a). In Cx3cr1-RasV12 mice, EGFP expression was detected in approximately 1% of CD11b-positive cells (Supplementary Fig. S1b). Therefore, we could confidently conclude that EGFP-positive cells in the retina and brain were mostly microglia and that the representation of macrophages in this population is negligible.

Characterization of RasV12-expressing microglia in the retina and brain

We then evaluated the presence of RasV12-expressing microglia in the retina and the brain. Retinas harvested at day 7 were frozen-sectioned for histological examination. The number of EGFP-positive cells was considerably higher in retinas from Cx3cr1-RasV12 mice compared with control retinas (Fig. 1a, c). Moreover, the vast majority of EGFP-expressing cells also expressed Iba1, which is a marker of microglia and macrophages (Fig. 1b). We then examined the time course of EGFP expression at days 1, 3, 5, and 7 after tamoxifen administration. EGFP was expressed from day 3 in the retinas of control and Cx3cr1-RasV12 mice (Fig. 1e, arrowheads). EGFP-positive cells also expressed the microglia-specific marker TMEM119 (Fig. 1e) [23]. $EGFP^+TMEM119^+$ cells accounted for nearly 90% of the total EGFP-positive cell population in control and Cx3cr1-RasV12 retinas at days 3, 5, and 7 after tamoxifen administration (Fig. 1F). The number of $EGFP^+TMEM119^+$ cells increased until day 7 in Cx3cr1-RasV12 retinas, whereas only a slight increase was observed in control retinas (Fig. 1e, g). Furthermore, immunohistochemical analysis revealed the presence of phosphorylated ERK1/2 in EGFP-positive microglia in Cx3cr1-RasV12 retinas (Fig. 1h, arrowheads), confirming Ras signaling pathway activation in these microglial cells.

In the brains of Cx3cr1-RasV12 mice, we observed prominent EGFP expression in the ventral orbital cortex (VO), lateral orbital cortex (LO), and ventral tenia tecta (VTT) at day 7 after tamoxifen administration (Supplementary Fig. Sa). Hematoxylin and eosin staining confirmed strong nuclear staining in these regions of the brain (Supplementary Fig. S2b). Similar to what we observed in the retina, EGFP expression was apparent from day 3 in the orbital cortex region of the brain (Supplementary Fig. S2c), and EGFP-positive cells also expressed Iba1 (Supplementary Fig. S2c, arrowheads d, e). The number of $EGFP^+Iba1^+$ cells continuously increased in the brain of Cx3cr1-RasV12 mice (Supplementary Fig. S2c, d). Moreover, ERK1/2 phosphorylation was detected in EGFP-positive cells in the brain of Cx3cr1-RasV12 mice (Supplementary Fig. S2f, arrowheads).

Migration and proliferation of RasV12-expressing microglia

Resting microglia are often found in the IPL and OPL of the retina [24]. In control retinas, $EGFP^+TMEM119^+$ cells were primarily found in the IPL and OPL at day 7 after tamoxifen administration (Fig. 1e, 2a). In contrast, RasV12-expressing microglia were observed in the ganglion cell layer (GCL), ONL, and SR (Fig. 1e, 2a), suggesting microglial cell migration to the apical and basal sides of the retina.

At day 7 after tamoxifen administration, retinas from Cx3cr1-RasV12 mice contained a significantly higher number of $EGFP^+TMEM119^+$ cells compared with control retinas (Fig. 1g). Additionally, retinas from Cx3cr1-RasV12 mice contained a significantly higher number of proliferating microglial cells ($Ki67^+EGFP^+$; Fig. 2b, arrow heads). $Ki67^+EGFP^+$ cells comprised nearly 70% of the total EGFP-positive

cell population in retinas from Cx3cr1-RasV12 mice (Fig. 2c). Although $Ki67^{+}EGFP^{+}$ cells were present in all retinal layers, notably high numbers were observed in the apical and basal regions (Fig. 2d).

RasV12-expressing microglia exhibited ameboid morphology with a large cell body and short pseudopodia (Fig. 2b), which is typically observed in activated microglia [25, 26]. Consistently, *Ccl2*, *Ccl3*, *Cxcl1*, *Cxcl5*, *Il1b, Il6*, and *Tnf* were significantly upregulated in Cx3cr1-RasV12 retinas (Fig. 2e), further supporting microglial activation (Nakagawa and Chiba, 2014; Franco and Fernández-Suárez, 2015). In the brain, although a significant number of EGFP-positive cells expressed Ki67 (Supplementary Fig. S3a, b), Ki67-positive cells comprised less than 30% of the total EGFP-positive cell population (Supplementary Fig. S3c).

RasV12 expression in microglia promotes photoreceptor degeneration

Histological analysis indicated the loss of photoreceptors in Cx3cr1-RasV12 retinas (Fig. 3a, arrowheads). Immunohistochemical staining revealed that microglial cells were localized close to the degenerating regions of the ONL (Fig. 3b). Moreover, differential interference contrast (DIC) imaging showed a reduction in the thickness of the outer layer of Cx3cr1-RasV12 retinas (Fig. 3b, c). We also performed Annexin V staining to measure apoptosis [29] and found an increased number of apoptotic cells in Cx3cr1-RasV12 retinas. Importantly, the number of apoptotic cells was higher in CD73-positive rod cells than other retinal cells (Fig. 3d, e). In Cx3cr1-RasV12 retinas, we also observed upregulation of *Edn2* and *Fgf2* (Fig. 3f), which are commonly induced upon photoreceptor damage [8].

Retinal degeneration is often accompanied by reactive gliosis, which is characterized by strong GFAP expression [30]. Consistently, GFAP was upregulated in Cx3cr1-RasV12 retinas (Fig. 3g, h), and microglia were localized adjacent to the GFAP-positive MGCs (Fig. 3f, enlarged panels). We found no differences in the numbers of RBPMS-positive retinal ganglion cells (Supplementary Fig. S4a), AP-2α-positive amacrine cells (Supplementary Fig. S4b), Chx10-positive bipolar cells (Supplementary Fig. S4c), and Calbindin-positive horizontal cells (Supplementary Fig. S4d) in RasV12-expressing and control retinas, suggesting that survival and maintenance of these cell types was not affected by RasV12 expression in microglia.

RasV12-expressing microglia in the ONL, but not in the INL, mediates rod photoreceptor phagocytosis

Confocal microscopy revealed that RasV12-expressing microglia engulfed recoverin-positive rod photoreceptors in the damaged ONL regions (Fig. 4a); hence, we measured phagocytosis related molecules in Cx3cr1-RasV12 retinas. In Cx3cr1-RasV12 mice, EGFP-positive cells strongly expressed CD68 (Fig. 4b, arrow heads), which is a lysosomal protein highly expressed in activated microglia [7, 31]. Interestingly, the number of CD68-expressing cells was higher in the ONL and SR than in the inner layers

of the retina (Fig. 4c). Furthermore, population of the $EGFP^+CD68^+TMEM119^+$ cells in EGFP and Tmem119 double positive cells was considerably higher in the ONL and SR than in other retinal regions (Fig. 4d). Microglial iNOS expression was demonstrated in rd8 mice[28, 32], and an optic nerve injury mouse model [33]. Immunohistochemical staining revealed strong iNOS expression in EGFP-positive microglial cells in Cx3cr1-RasV12 retinas (Fig. 4e). $EGFP^+iNOS^+$ cells were also observed in the inner retinal layers (Fig. 4e, f); nevertheless, this double-positive cell population was higher in the ONL and SR than in other regions of the retina (Fig. 4g). Furthermore, the phagocytosis-related genes *C3* and *Cd68* were upregulated in Cx3cr1-RasV12 retinas (Fig. 4h).

The behavior of RasV12-expressing microglia differs in the IPL and ONL

We next examined the behavior of RasV12-expressing microglia in different regions of the retina. We prepared retinal explants from Cx3cr1-RasV12 mice and labeled the nuclei of rod photoreceptors with Hoechst33342. Time-lapse imaging revealed that RasV12-expressing microglia in the ONL engulfed photoreceptors by extending their pseudopodia. Moreover, multiple nuclei were observed in individual microglial cells, suggesting rod photoreceptor engulfment by microglia (Fig. 5, upper panel, Supporting information movie 1). However, we found no evidence of cells engulfment by RasV12-expressing microglia in the IPL (Fig. 5, lower panel, Supporting information movie 2).

Discussion

In this study, we examined the role of Ras activation in retinal microglia by inducing the expression of constitutively active Ras (RasV12) in microglial cells. RasV12 expression promoted microglial activation, as well as activation of MGCs, which led to the degeneration of retinal photoreceptors. Previous studies highlighted the importance of FGF2, EDN2, LIF, and other inflammatory cytokines in retinal degeneration. Consistently, we found that *Gfap*, *Edn2*, and *Fgf2* were upregulated in Cx3cr1-RasV12 retinas, suggesting that microglial activation results in cytokine secretion.

Most studies on the molecular mechanisms of microglia involved the use of photoreceptor degeneration models, suggesting that the initial event of inflammatory cascade is photoreceptor injury. *Edn2* upregulation has been reported in injured photoreceptors, and EDN2 contributes to the activation of MGCs [9]; however, the mechanisms regulating its transcriptional activation remain elusive. Similarly, transcription of *Lif* is induced upon tissue damage, and its expression induces activation of MGCs, characterized by GFAP expression. In this study, we found evidence of *Edn2* and *Lif* transcriptional activation in Cx3cr1-RasV12 retinas. Therefore, RasV12 expression in microglia is sufficient to induce *Edn2* expression in the absence of injury of photoreceptors, and in photoreceptor degeneration mouse models, *Edn2* upregulation is likely induced at least partly by microglia. Alarmin is expressed at the initial phase of photoreceptor degeneration, and it may contribute to microglial activation early during degeneration. On the other hand, EDN2 is known to exerts protective effects on photoreceptors. Therefore,

microglia may modulate retinal degeneration protectively through up-regulation of EDN2 on rod photoreceptors in certain situation.

BRAFV600E mutation has been implicated in late-onset neurodegenerative diseases and histiocytosis [34, 35]. Mosaic expression of BRAFV600E in the yolk-sac erythro-myeloid progenitors resulted in clonal expansion of microglia and late-onset neurodegeneration in the brain [16]. Our RasV12 microglial activation model shared some features with this BRAFV600E-expressing model, including the expansion of Iba1-positive cells, GFAP expression, and inflammatory cytokine expression. However, our RasV12-expressing microglia mouse model exhibited early-onset microglial activation in the brain and neural degeneration in the retina. Furthermore, our mice did not survive more than nine days after tamoxifen administration. On the other hand, no description about early phenotype of BRAFV600E expressing model was available; therefore, we could not directly compare the findings acquired from these two animal models. Considering that Ras acts upstream of BRAF and activates not only the MAPK pathway but also multiple other signaling pathways, it is not surprising that our RasV12-expressing microglia model has a more complex phenotype than the BRAFV600E-expressing model.

Interestingly, Ras activation in microglia resulted in cell migration towards the apical and basal regions of the retina. Because ERK1/2 activates various migration-related molecules, such as MLCK, Paxillin, FAK, and Calpain [36], the enhanced migration of RasV12-expressing microglia was anticipated; however, we could not explain the tropism observed in microglia migration patterns. In photoreceptor degeneration models, microglia migrated primarily in degeneration sites; however, the molecules promoting cell migration could not be identified. In this study, we found that RasV12-expressing microglia were localized close to MGCs; thus, it is likely that microglial cells migrated along the migration pathway of MGCs. However, no determinant of apical or basal direction is hypothesized currently, and diffused migration is rather plausible.

Nitric oxide has been identified as one of the mediators of the cytotoxic effects of activated microglia [37]. Consistently, we observed enhanced expression of iNOS and inflammatory cytokines in RasV12-expressing microglia. These inflammatory stimuli may have contributed to rod photoreceptor apoptosis and subsequent phagocytosis by RasV12-expressing microglia. Interestingly, although iNOS upregulation was also observed in RasV12-expressing microglia in the GCL and IPL, we could not detect degeneration of non-photoreceptor cells or phosphatidylserine (PS) expression on CD73-negative cells in Cx3cr1-RasV12 retinas. Moreover, the cellular dynamics of RasV12-expressing microglia were profoundly different in the ONL and IPL. These results suggest that rod photoreceptors are targeted by activated microglia.

Conclusions

In summary, our data suggested that activation of Ras signaling in the microglia induced not only microglial proliferation, changing distribution, and increasing phagocytotic activity but also photoreceptor degeneration. Furthermore, cellular dynamics of RasV12-expressing microglia were different between in

ONL and IPL. Therefore, constitutive microglial activation induced retinal degeneration and microenvironment cues may modulate the microglial phenotypic features and effects of microglial activation. Future studies are required to examine the role of the immunosuppressive microenvironment of the inner side of the retina.

Abbreviations

CSF1R, colony stimulating factor 1 receptor; DIC, differential interference contrast; FcγR, fc gamma receptor; GCL, ganglion cell layer; INL, inner nuclear layer; IPL, inner plexiform layer; LIF, leukemia inhibitory factor; LO, lateral orbital cortex; MGCs, Müller glial cells; ONL, outer nuclear layer; PS, phosphatidylserine; RPE, retinal pigment epithelium; SR, subretinal regions; VO, ventral orbital cortex; VTT, ventral tenia tecta

Declarations

The all authors have nothing to declare regarding following issues.

Ethics approval and consent to participate;

not applicable

Consent for publication;

not applicable

Availability of data and materials;

The datasets used and/or analysed during the current study are available from the corresponding authors on reasonable request.

Competing interests;

All authors have nothing to declare on this issue.

Funding;

This work is supported by the grants from MEXT, Japan.

Authors' contributions;

YM and SW planned the experiments.

YM performed experiments.

YM, TI, HK, and SW analyzed an interpreted the data.

AT performed the histological examination.

YF provided critical mouse model.

YM and SW wrote manuscript.

Acknowledgements;

We thank Miho Nagoya for excellent technical assistance and Yukihiro Baba for fruitful discussion.

References

1. Kierdorf K, Prinz M. Microglia in steady state. J Clin Invest. 2017;127:3201–9.
2. Salter MW, Stevens B. Microglia emerge as central players in brain disease. Nat Med. 2017;23:1018–27.
3. Silverman SM, Wong WT. Microglia in the Retina: Roles in Development, Maturity, and Disease. Annu Rev Vis Sci. 2018;4:45–77. doi:10.1146/annurev-vision-091517-034425.
4. Santos AM, Martín-Oliva D, Ferrer-Martín RM, Tassi M, Calvente R, Sierra A, et al. Microglial response to light-induced photoreceptor degeneration in the mouse retina. J Comp Neurol. 2010;518:477–92.
5. Ng TF, Streilein JW. Light-induced migration of retinal microglia into the subretinal space. Investig Ophthalmol Vis Sci. 2001;42:3301–10.
6. Zhao L, Zabel MK, Wang X, Ma W, Shah P, Fariss RN, et al. Microglial phagocytosis of living photoreceptors contributes to inherited retinal degeneration. EMBO Mol Med. 2015;7:1179–97. doi:10.15252/emmm.201505298.
7. Tipoe GL, Wang K, Lin B, Xiao J, So K-F, Peng B. Suppression of Microglial Activation Is Neuroprotective in a Mouse Model of Human Retinitis Pigmentosa. J Neurosci. 2014;34:8139–50.
8. Rattner A. The Genomic Response to Retinal Disease and Injury: Evidence for Endothelin Signaling from Photoreceptors to Glia. J Neurosci. 2005;25:4540–9. doi:10.1523/JNEUROSCI.0492-05.2005.
9. Joly S, Lange C, Thiersch M, Samardzija M, Grimm C. Leukemia Inhibitory Factor Extends the Lifespan of Injured Photoreceptors In Vivo. J Neurosci. 2008;28:13765–74. doi:10.1523/JNEUROSCI.5114-08.2008.

10. Ueki Y, Wang J, Chollangi S, Ash JD. STAT3 activation in photoreceptors by leukemia inhibitory factor is associated with protection from light damage. J Neurochem. 2008;105:784–96.
11. Holtkamp GM, Kijlstra A, Peek R, De Vos AF. Retinal pigment epithelium-immune system interactions: Cytokine production and cytokine-induced changes. Prog Retin Eye Res. 2001;20:29–48.
12. Simanshu DK, Nissley D V., McCormick F. RAS Proteins and Their Regulators in Human Disease. Cell. 2017;170:17–33. doi:10.1016/j.cell.2017.06.009.
13. Pixley FJ, Stanley ER. CSF-1 regulation of the wandering macrophage: Complexity in action. Trends Cell Biol. 2004;14:628–38.
14. Song X, Tanaka S, Cox D, Lee SC. Fcγ receptor signaling in primary human microglia: differential roles of PI-3K and Ras/ERK MAPK pathways in phagocytosis and chemokine induction. J Leukoc Biol. 2004;75:1147–55. doi:10.1189/jlb.0403128.
15. Colonna M, Wang Y. TREM2 variants: New keys to decipher Alzheimer disease pathogenesis. Nat Rev Neurosci. 2016;17:201–7.
16. Mass E, Jacome-Galarza CE, Blank T, Lazarov T, Durham BH, Ozkaya N, et al. A somatic mutation in erythro-myeloid progenitors causes neurodegenerative disease. Nature. 2017;549:389–93. doi:10.1038/nature23672.
17. Yona S, Kim KW, Wolf Y, Mildner A, Varol D, Breker M, et al. Fate Mapping Reveals Origins and Dynamics of Monocytes and Tissue Macrophages under Homeostasis. Immunity. 2013;38:79–91. doi:10.1016/j.immuni.2012.12.001.
18. Kon S, Ishibashi K, Katoh H, Kitamoto S, Shirai T, Tanaka S, et al. Cell competition with normal epithelial cells promotes apical extrusion of transformed cells through metabolic changes. Nat Cell Biol. 2017;19:530–41.
19. Kawamoto S, Niwa H, Tashiro F, Sano S, Kondoh G, Takeda J, et al. A novel reporter mouse strain that expresses enhanced green fluorescent protein upon Cre-mediated recombination. FEBS Lett. 2000;470:263–8.
20. Koso H, Tsuhako A, Lai CY, Baba Y, Otsu M, Ueno K, et al. Conditional rod photoreceptor ablation reveals Sall1 as a microglial marker and regulator of microglial morphology in the retina. Glia. 2016;64:2005–24.
21. Wolf Y, Yona S, Kim K-W, Jung S. Microglia, seen from the CX3CR1 angle. Front Cell Neurosci. 2013;7 March:1–9.
22. Landsman L, Liat BO, Zernecke A, Kim KW, Krauthgamer R, Shagdarsuren E, et al. CX3CR1 is required for monocyte homeostasis and atherogenesis by promoting cell survival. Blood. 2009;113:963–72.
23. Bennett ML, Bennett FC, Liddelow SA, Ajami B, Zamanian JL, Fernhoff NB, et al. New tools for studying microglia in the mouse and human CNS. Proc Natl Acad Sci. 2016;113:E1738–46. doi:10.1073/pnas.1525528113.
24. Rashid K, Akhtar-Schaefer I, Langmann T. Microglia in retinal degeneration. Front Immunol. 2019;10 AUG:1–19.

25. Rathnasamy G, Foulds WS, Ling EA, Kaur C. Retinal microglia – A key player in healthy and diseased retina. Prog Neurobiol. 2018; March:1–23. doi:10.1016/j.pneurobio.2018.05.006.
26. Ulland TK, Song WM, Huang SCC, Ulrich JD, Sergushichev A, Beatty WL, et al. TREM2 Maintains Microglial Metabolic Fitness in Alzheimer's Disease. Cell. 2017;170:649-663.e13. doi:10.1016/j.cell.2017.07.023.
27. Nakagawa Y, Chiba K. Role of microglial M1/M2 polarization in relapse and remission of psychiatric disorders and diseases. Pharmaceuticals. 2014;7:1028–48.
28. Franco R, Fernández-Suárez D. Alternatively activated microglia and macrophages in the central nervous system. Prog Neurobiol. 2015;131:65–86.
29. Vermes I, Haanen C, Steffens-Nakken H, Reutellingsperger C. A novel assay for apoptosis Flow cytometric detection of phosphatidylserine expression on early apoptotic cells using fluorescein labelled Annexin V. J Immunol Methods. 1995;184:39–51.
30. Ekstrom P, Sanyal S, Narfstrom K, Chader GJ, Van Veen T. Accumulation of glial fibrillary acidic protein in Muller radial glia during retinal degeneration. Investig Ophthalmol Vis Sci. 1988;29:1363–71.
31. Amadio S, Parisi C, Montilli C, Carrubba AS, Apolloni S, Volonté C. P2Yreceptor on the verge of a neuroinflammatory breakdown. Mediators Inflamm. 2014;2014.
32. Aredo B, Zhang K, Chen X, Wang CXZ, Li T, Ufret-Vincenty RL. Differences in the distribution, phenotype and gene expression of subretinal microglia/macrophages in C57BL/6N (Crb1rd8/rd8) versus C57BL6/J (Crb1wt/wt) mice. J Neuroinflammation. 2015;12:4–17.
33. Noro T, Namekata K, Kimura A, Guo X, Azuchi Y, Harada C, et al. Spermidine promotes retinal ganglion cell survival and optic nerve regeneration in adult mice following optic nerve injury. Cell Death Dis. 2015;6:1–9.
34. Haroche J, Charlotte F, Arnaud L, Von Deimling A, Hélias-Rodzewicz Z, Hervier B, et al. High prevalence of BRAF V600E mutations in Erdheim-Chester disease but not in other non-Langerhans cell histiocytoses. Blood. 2012;120:2700–3.
35. Berres ML, Lim KPH, Peters T, Price J, Takizawa H, Salmon H, et al. BRAF-V600E expression in precursor versus differentiated dendritic cells defines clinically distinct LCH risk groups. J Exp Med. 2014;211:669–83.
36. Huang C. MAP kinases and cell migration. J Cell Sci. 2004;117:4619–28. doi:10.1242/jcs.01481.
37. Block ML. Neuroinflammation: Modulating mighty microglia. Nat Chem Biol. 2014;10:988–9. doi:10.1038/nchembio.1691.

Figures

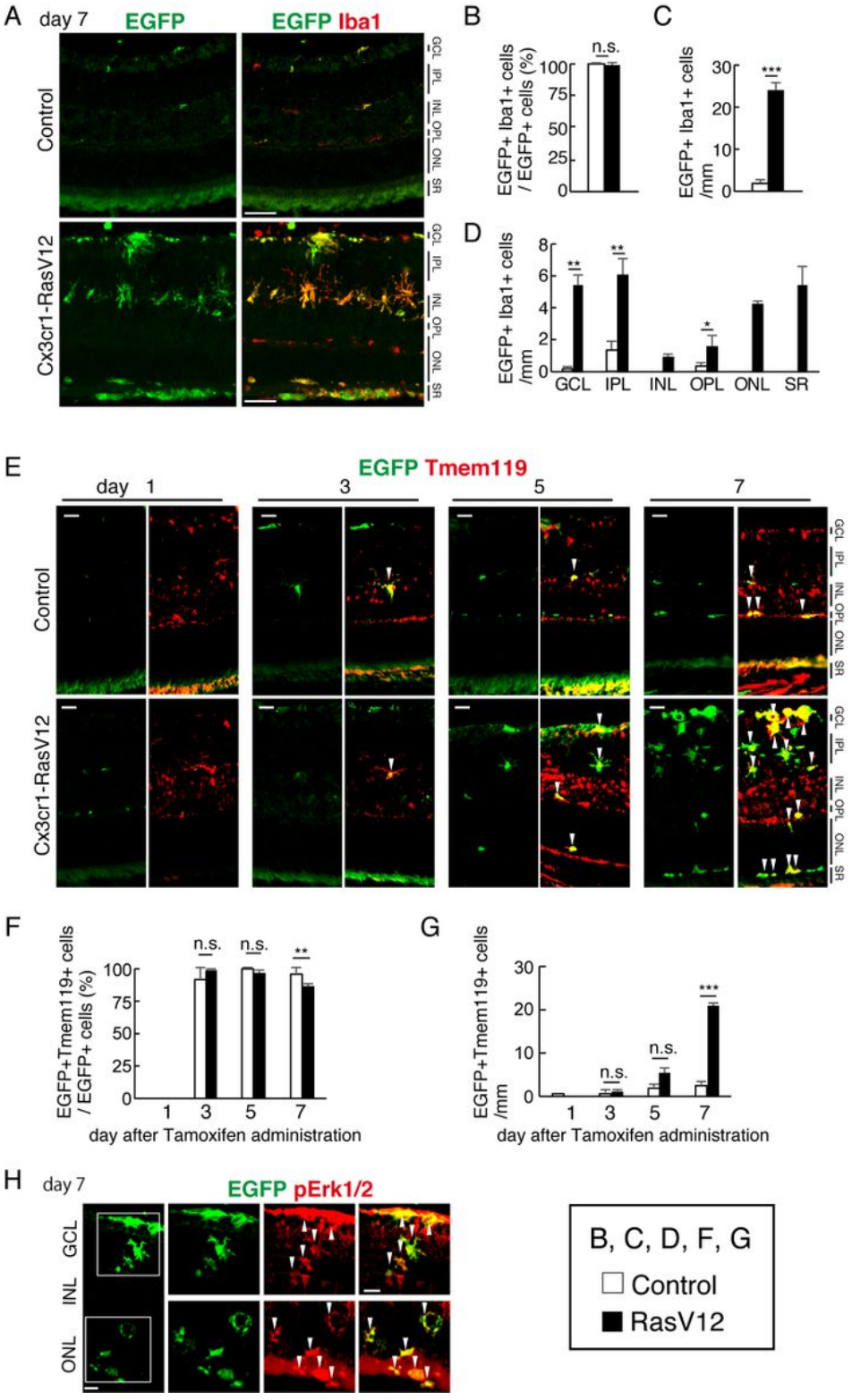

Figure 1

Expression of RasV12-EGFP in the microglia in Cx3cr1-RasV12 mouse a-d Cx3cr1-RasV12 or control mice at P14 were injected with tamoxifen, and after day (s) 1, 3, 5, and 7, the retinas were harvested. Isolated retinas were frozen sectioned, and stained with anti-EGFP and indicated antibodies. a EGFP and Iba1 double staining patterns of day 7 retinas. b The population of EGFP and Iba1 double positive cells in total EGFP positive cells. c The number of EGFP and Iba1 double positive cells at day 7. d Distribution of EGFP

and Iba1 double positive cells in retinal layers. e EGFP and Tmem119 double staining patterns in day 1, 3, 5, and 7 after tamoxifen administration. f The population of EGFP and Tmem119 doble positive cells in total EGFP positive cells. g The number of double positive cells. (h) EGFP and phosphorylated Erk1/2 (pErk1/2) patterns at day7. Scale bars, 20 μm. Graphs are average of 3 samples from independent mice with SEM. * p<0.05, ** p<0.01, *** p <0 .001 by unpaired t-tests. ganglion cell layer; GCL, inner plexiform layer; IPL, inner nuclear layer; INL, outer plexiform layer; OPL, outer nuclear layer; ONL, subretinal regions; SR.

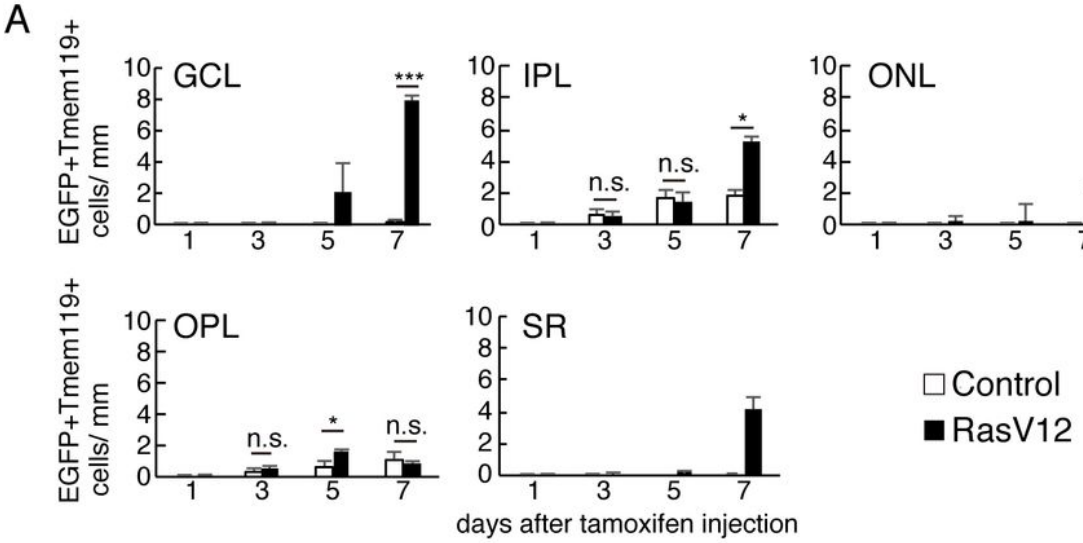

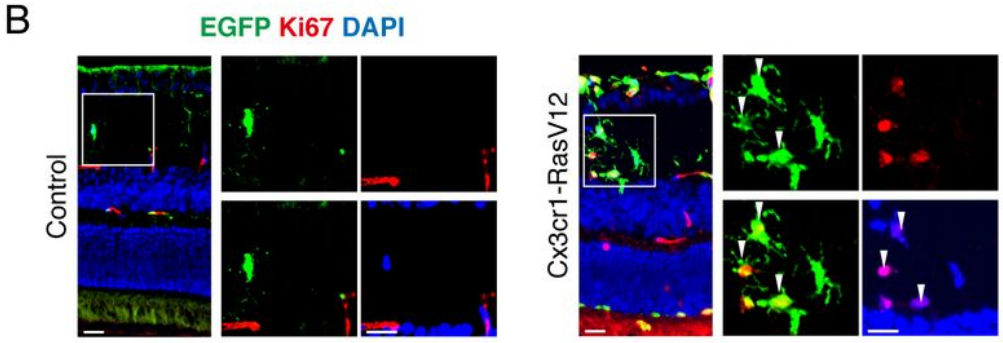

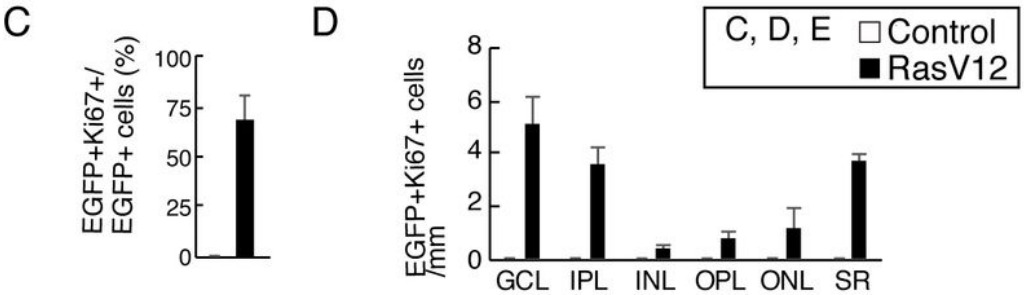

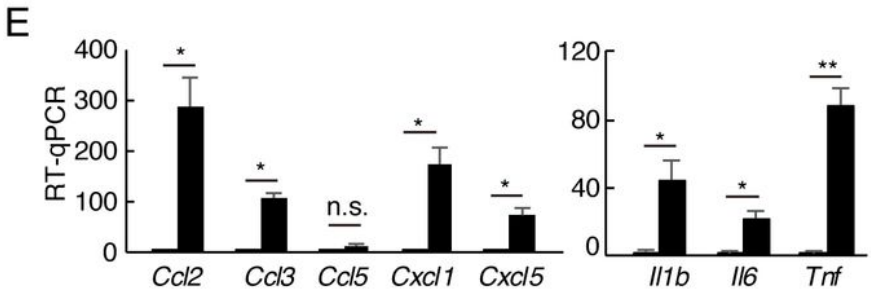

Figure 2

RasV12 expressing microglia accumulated in both basal and apical sides of the retina a Distribution of RasV12/EGFP or control EGFP expressing-microglia in the retina. Related to Fig.1e. Quantification of number of EGFP and Tmem119 double positive cells in ganglion cell layer (GCL), inner plexiform layer (IPL), outer nuclear layer (ONL), and subretinal regions (SR) are shown. (B-D) Proliferation of the microglia was examined by the immunohistochemical analysis of Ki67. b Immunostaining patterns of anti-EGFP and -Ki67 antibodies of day 7 retinas. Nuclei were visualized with staining by DAPI. c The Population of EGFP and Ki67 double positive cells in total EGFP positive cells. d Distribution of EGFP and Ki67 double positive cells. e Expression of transcripts of various chemokines and cytokines were examined by RT-qPCR from total RNA from retinas of Cx3cr1-RasV12 or control mice at day 7 after tamoxifen administration. a, c, d, and, e are average with SEM from 3 samples of independent mice. * $p<0.05$, ** $p<0.01$, *** $p <0 .001$by unpaired t-tests.

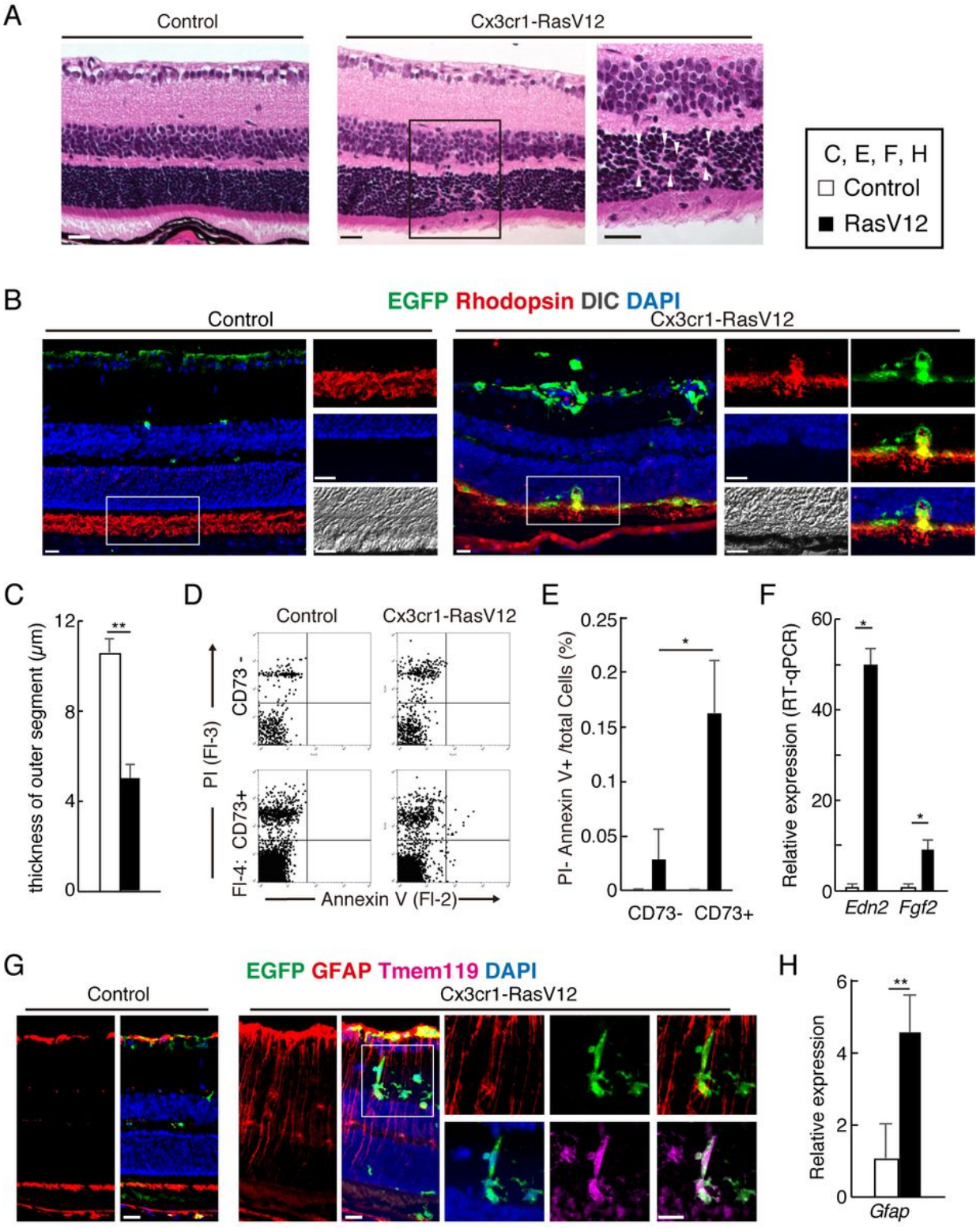

Figure 3

Perturbed ONL structure and activated Müller glia in Cx3cr1-RasV12 retina a Paraffin sectioned retinas of control or Cx3cr1-RasV12 mice were subjected to HE staining. Right panel of Cx3cr1-RasV12 section is enlarged view of black squared region in the middle panel. White arrowheads indicate spotted missing of photoreceptors. Scale bars, 20 μm. b Frozen sectioned retinas of control or Cx3cr1-RasV12 were subjected to immunohistochemistry using anti-EGFP, -Rhodopsin antibody, and differential interference

contrast (DIC) imaging. Nuclei were visualized by staining with DAPI. Scale bars, 20 μm. c Thickness of outer-segment was measured from DIC pictures in control and Cx3cr1 mice retina. d, e Flow cytometrical analysis of retinal cells of control and Cx3cr1-RasV12 retinas by staining with Annexin V, CD73, and PI. Dot blot patterns of Annexin V and Propidium iodide (PI) of CD73 negative (upper panels) and CD73 negative (lower panels) are shown. PI negative/Annexin V positive cell population in CD73 negative and positive population of Cx3cr1-RasV12 retina are shown. f Expression levels of Edn2 and Fgf2 transcripts by RT-qPCR in control and Cx3cr1-RasV12 retinas at day 7. g Frozen sections of control of Cx3cr1-RasV12 mice derived retinas were stained with anti-EGFP, -GFAP, and -Tmem119 antibodies. Nuclei were visualized with DAPI staining. h The expression level of Gfap transcripts of control or Cx3cr1-RasV12 retina was examined by RT-qPCR. In c, f, and h the graphs are average of 3 independent samples with SEM. In e, the graphs are average of 4 independent samples with SEM. *$p<0.05$, ** $p< 0.01$ by unpaired t-tests.

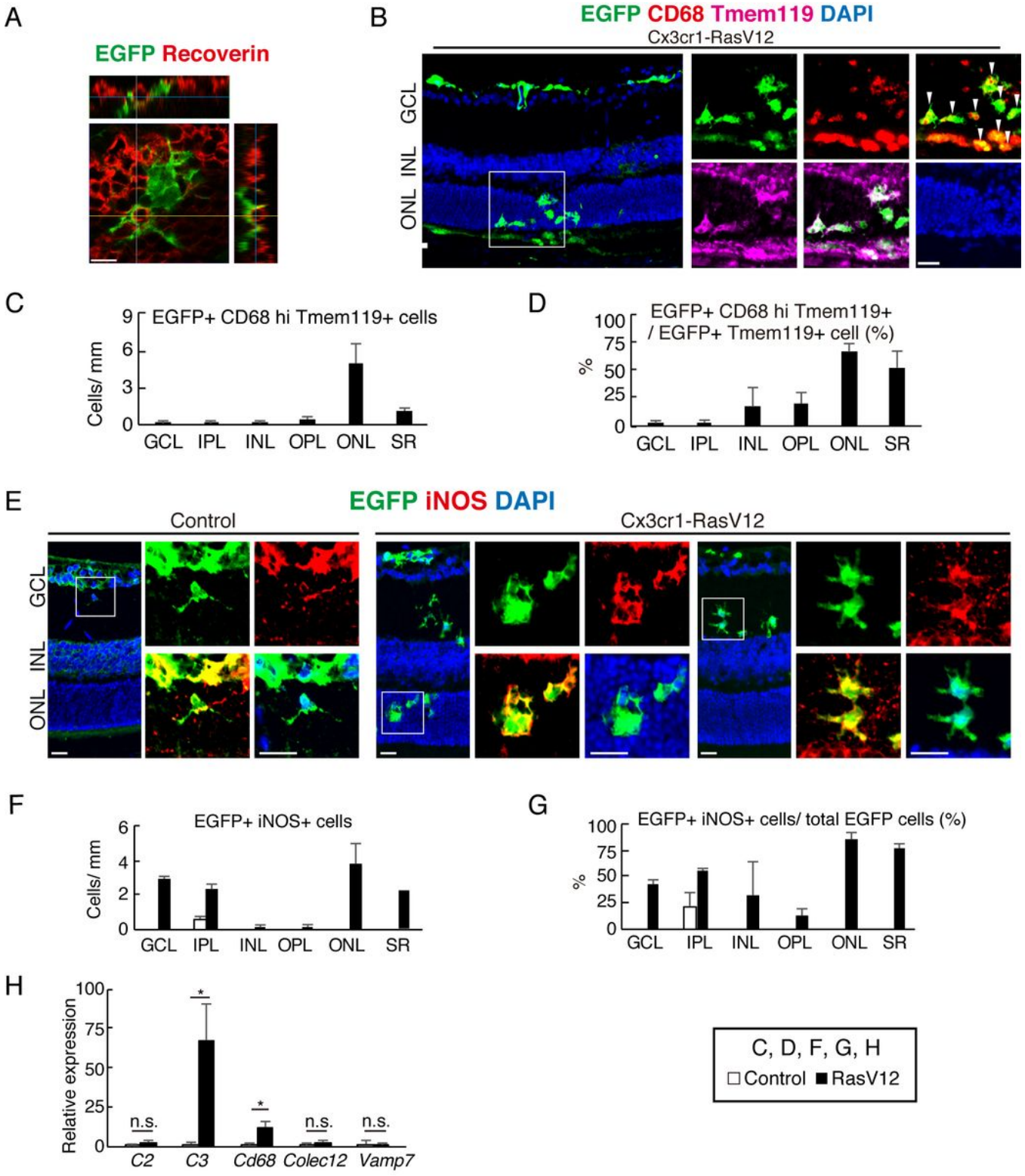

Figure 4

The expression of phagocytosis related molecules in Cx3cr1-RasV12 mice retina aOrthological view of EGFP and Recoverin stained retina of Cx3cr1-RasV12 mice at day 7. Scale bar, 10 μm. b-d Frozen sectioned retinas of control and Cx3cr1-RasV12 mice at day 7 after tamoxifen injection were subjected to immunohistochemistry using anti-EGFP, -CD68, and -Tmem119 antibodies. Nuclei were visualized with DAPI in some panels. White arrowheads indicate EGFP, CD68 and Tmem119 triple positive cells in ONL.

Scale bar, 20 μm. c Number of EGFP, CD68, and Tmem119 triple positive cells in sub-regions of the retina was counted, and cell number in each sub-region in 1mm width of the section. d The population of the triple positive cells in EGFP and Tmem119 double positive cells (%) in sub-regions of the retina. e-g Frozen sectioned retinas of control and Cx3cr1-RasV12 mice at day 7 after tamoxifen injection were stained with anti-EGFP, and -iNOS antibodies. Nuclei were visualized with DAPI in some panels. White arrowheads indicate EGFP and iNOS double positive cells. Scale bars, 20 μm. f Number of EGFP and iNOS double positive cells in sub-regions of retina was counted. g The population of the double positive cells in total EGFP positive cells (%). h Expression of transcripts of various phagocytosis related genes in control and Cx3cr1-RasV12 retina were examined by RT-qPCR. c, d, f, g, and h; Data are average of counting from 3 independent samples with SEM. ganglion cell layer; GCL, inner plexiform layer; IPL, inner nuclear layer; INL, outer plexiform layer; OPL, outer nuclear layer; ONL, subretinal regions; SR.

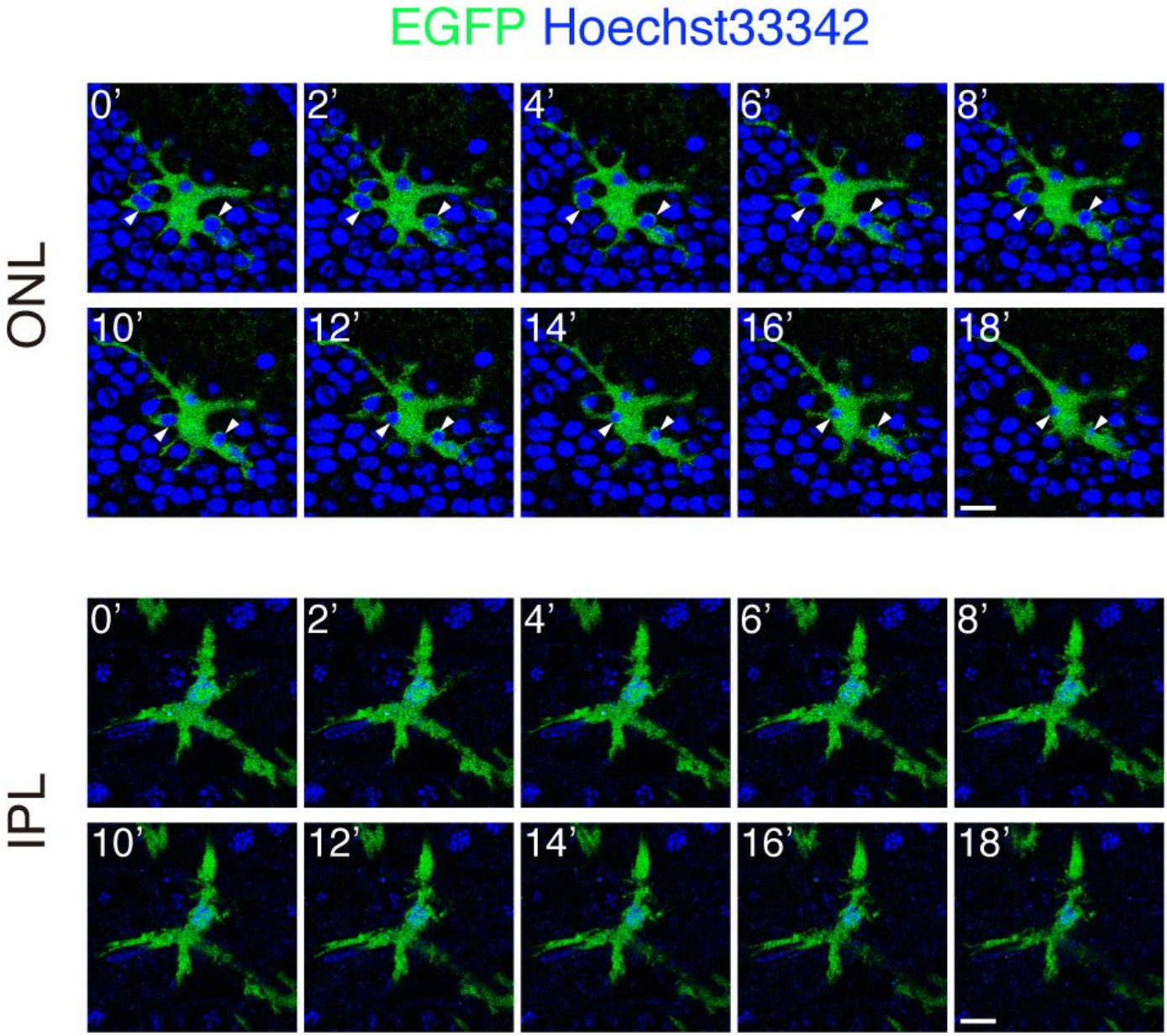

Figure 5

Phagocytosis of photoreceptors by RasV12-expressing microglia were observed in ONL but not observed in IPL. Time-lapse analysis in Cx3cr1-RasV12 retinal explant. EGFP positive cell phagocytosed nuclear in ONL (upper panels) but did not show phagocytotic activity in IPL (lower panels). White arrow heads indicate phagocytosed nuclei by EGFP positive cell. Panels show pictures in 2 min intervals. Scale bars, 10μm. Movies are up-loaded as supporting information.

Supplementary Files

This is a list of supplementary files associated with this preprint. Click to download.

- SupportinginformationMovie1ONLtimelapse.mp4
- SupplementalfiguresMoriuchietal.pdf
- DearEditor.docx
- SupportinginformationMovie2IPLtimelapse.mp4